

# Diode-pumped passively mode-locked laser using SHG in periodically poled crystals

Hristo Iliev,<sup>a)</sup> Danail Chuchumishev,<sup>a)</sup> Ivan Buchvarov,<sup>a)</sup> Valentin Petrov<sup>b)</sup>

<sup>a)</sup>Faculty of Physics, Department of Quantum Electronics, Sofia University, 5 James Bourchier Blvd.,

BG-1164 Sofia, Bulgaria

<sup>b)</sup>Max-Born-Institute for Nonlinear Optics and Ultrafast Spectroscopy, 2A Max-Born-Str.,

D-12489 Berlin, Germany

## ABSTRACT

Experimental results on passive mode-locking of Nd: YVO<sub>4</sub> laser using intracavity frequency doubling in periodically poled KTP (PPKTP) crystal is reported. Both, negative cascaded chi-2 lensing and frequency doubling nonlinear mirror (FDNLM) are exploited for the laser mode-locking. The FDNLM based on intensity dependent reflection in the laser cavity ensures self-starting and self-sustaining mode-locking while the cascaded chi-2 lens process contributes to the substantial pulse shortening. This hybrid technique enables generation of stable trains of pulses at high-average output power with several picoseconds pulse width. The pulse repetition rate of the laser is 117 MHz with average output power ranging from 0.5 W to 3.1 W and pulse duration from 2.9 to 5.2 ps.

Key words: Diode pumped lasers, passive mode-locking, quasi-phase matching, periodically-poled crystals

## 1. INTRODUCTION

Since its discovery in 1966 passive mode-locking<sup>1</sup> as a technique for generation of ultrashort laser pulses has been under continuous development implementing it with any newly developed solid state laser material. During the last decade the strong interest in mode-locked lasers received an additional impact with the development of reliable and efficient pump laser diodes.<sup>2</sup> Such diode pumped all solid state lasers show enhanced reliability and unprecedented performance. Diode pumped mode-locked neodymium lasers generate pulses in the range of 2-100 ps at ~100 MHz repetition rate, producing high peak and high average power<sup>2-5</sup>. These lasers are particularly attractive for nonlinear optics, spectroscopy, and other applications such as medical diagnostics and micro-machining. Multi-watt operation of picosecond diode-pumped neodymium lasers based on passive mode-locking has been demonstrated mainly by two methods, one based on semiconductor saturable absorber mirrors (SESAMs)<sup>6-8</sup> and the other on intracavity frequency doubling. Although SESAMs are well established technology for lasers emitting around 1 μm, their residual absorption leading to heating is a major intrinsic drawback lowering their damage threshold (current state of the art is ~0.5 GW/cm<sup>2</sup> at 20 ps pulse duration)<sup>7</sup>. Hence, the power scaling capabilities of such systems are limited. On the other hand, using intracavity frequency doubling is a promising mode-locking approach for up-scaling the power of ultrashort pulse solid-state lasers. The damage threshold of the nonlinear crystals is an order of magnitude higher than SESAMs and the low absorption at the fundamental wave enables operation at high-average power. Furthermore, this approach is easily extendable to any spectral region. In the case of intracavity type-I second-harmonic generation (SHG), two different passive mode-locking mechanisms can be utilized. The first one is based on the intensity dependent reflectivity of the FDNLM, consisting of a

crystal for SHG and a dielectric mirror<sup>9-12</sup>. In this scheme the second harmonic generated upon passing through the nonlinear crystal is completely reflected by the dielectric mirror and interacts again with the fundamental on its way back through the same nonlinear crystal, thus a double-pass (cascaded) SHG process takes place. The dielectric mirror should be a dichroic mirror, having comparatively low reflection coefficient at the fundamental and high reflectivity at the second harmonic. Hence, the reflection coefficient of the assembly, crystal for SHG and a dielectric mirror, is governed by the back conversion from second harmonic to the fundamental<sup>11,13</sup>. The main drawback of the FDNLM is the longer duration of the output pulse in comparison with the pulse traveling inside the laser cavity.<sup>14</sup> The second mode-locking mechanism is based on cascaded  $\chi^{(2)}$  lens formation.<sup>3,15</sup> It does not exhibit the pulse duration limitation characteristic for the FDNLM. Thus it provides shorter pulses but higher nonlinearity is required for self-starting mode-locking. Also, this technique is sensitive to external perturbations. In this respect, cascaded  $\chi^{(2)}$  lens mode-locking assisted by FDNLM has a potential which has not been exploited effectively, yet. Moreover, the potential of quasi-phase-matched materials with their high effective nonlinearity and absence of spatial walk-off seems not to have been properly utilized. There are only a few reports in which SHG in periodically poled KTP (PPKTP) has been employed for passive mode-locking.<sup>9,14</sup>

In this work we investigate passive mode-locking of a Nd: YVO<sub>4</sub> laser using intracavity SHG in PPKTP. The FDNLM initiates the passive mode-locking process and ensures self-sustained operation while the defocusing cascaded  $\chi^{(2)}$  effect leads to the shortest pulse duration of 2.9 ps. Thus, although each of the two mode-locking mechanisms in principle can be used alone for passive mode-locking of the laser, the hybrid scheme proves beneficial for the robust laser performance in this study. The output power is ranging from 0.5 W to 3.1 W, close to the maximum value for TEM<sub>00</sub> CW operation of the laser.

## 2. EXPERIMENTAL SETUP

We use a 1.4 m long linear laser cavity for mode-locked operation (Fig. 1). The active element (AE) is a 5-mm long, a-cut, 1.5°-wedged Nd: YVO<sub>4</sub> crystal with 0.5 at. % doping, pumped by a 50-W 808-nm laser diode bar coupled in a 400  $\mu$ m optical fiber (NA=0.22). Its aperture is 2.5×2.5 mm<sup>2</sup> and the AE is mounted in a metal holder held at a temperature of 25°C by running water. The resonator end mirrors are the high-reflective rear face of the AE and the flat output coupler (OC). The other face of the AE is antireflection coated. The radius of curvature of the folding mirror M1 and the focal length of the lens F3 (80 mm) are chosen to ensure beam radius of 80  $\mu$ m in the nonlinear crystal (NLC) and 200  $\mu$ m in the AE. Single transverse mode operation is achieved by overlapping the resonator eigenmode with the pump waist which is formed using the objective lenses F1 and F2.

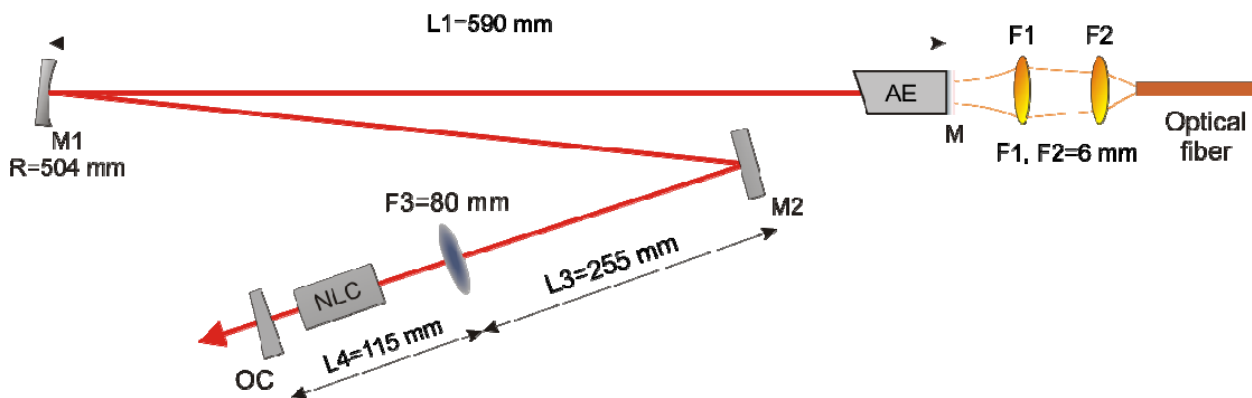


Fig. 1. Schematic of the laser cavity: F1, F2 – pump objective; AE - Nd: YVO<sub>4</sub> active element; M, M1, M2 – highly reflecting mirrors at the fundamental wavelength, F3 - focusing lens, NLC - PPKTP nonlinear crystal, OC - output coupler

After initial alignment of the laser oscillator, the distance between lens F3 and output coupler OC was optimized in order to achieve maximum output power in the fundamental transverse mode - TEM<sub>00</sub>. The laser operates in  $\pi$ -polarization. The distance between the NLC and OC was set around 25 mm. It was optimized for each mode-locking experiment by translating the NLC in order to achieve self-starting and continuous mode-locked operation. The NLC is a 1- mm thick PPKTP crystal with 8.94  $\mu\text{m}$  period, a length of 5 mm and a width of 5 mm, antireflection coated for both the fundamental and the second harmonic. It was mounted in an oven, which controls the temperature with an accuracy of 0.1°C.

### 3. MODE-LOCKING TECHNIQUE

The intracavity type-I SHG provides two different types of passive mode-locking mechanisms: The first one is based on the intensity dependent reflectivity of the FDNLM and the second one is based on cascaded  $\chi^{(2)}$  nonlinear phase shift of the fundamental wave, i.e. in this case cascaded  $\chi^{(2)}$  lens mode-locking is occurred.

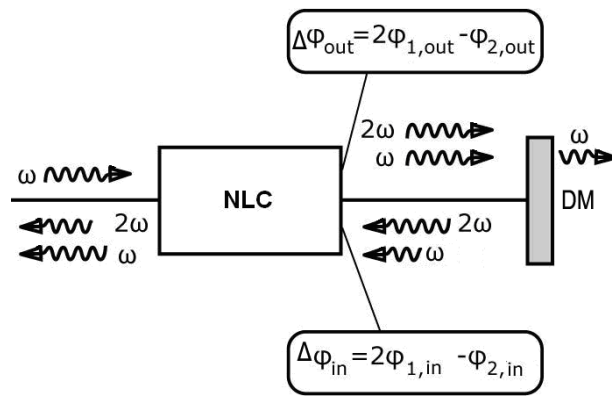


Fig. 2. Schematic of the FDNLM: NLC, nonlinear SHG crystal; DM, dichroic mirror.

A schematic of the FDNLM is shown on Fig. 2. The FDNLM consists of a frequency doubling nonlinear crystal (NLC) and a dichroic mirror (high reflecting at the second harmonic ( $2\omega$ ) and partially reflecting at the fundamental ( $\omega$ ) wavelength). In general, the reflection by the FDNLM includes a two-way pass of the beam through the frequency doubling nonlinear crystal. At perfect phase-matching of the SHG, the FDNLM reflection is governed by the conversion efficiency in the NLC which is a function of the input beam intensity and the phase difference  $\Delta\phi_{in} = 2\phi_{1,in} - \phi_{2,in}$  between the fundamental and second harmonic wave in the beginning of the second pass through the nonlinear crystal. If  $\Delta\phi_{in} = \Delta\phi_{out} \pm (2m+1)\pi$ ,  $m=0,1,2,\dots$ , the second harmonic is partially reconverted into the fundamental on the way back, leading to increase of the FDNLM reflectivity at the fundamental wavelength. The higher the intracavity intensity, the higher is the FDNLM reflectivity with respect to the fundamental wave. If the DM reflects partially the fundamental wave, the value of the FDNLM reflectivity can be higher than the value of the linear reflectivity of this mirror. Thus the FDNLM introduces a positive nonlinear feedback into the laser resonator. The nonlinear reflectivity  $R_{NL}$  normalized to the reflectivity  $R_{\omega}$  of the dichroic mirror is shown on Fig. 3a as a function of the single pass SHG efficiency. In the case of  $\Delta\phi_{in} = \Delta\phi_{out} \pm 2m\pi$ ,  $m=0,1,2,\dots$ , in the second pass through the nonlinear crystal, the phase difference  $\Delta\phi_{in}$  between the fundamental and the second harmonic waves enables further conversion of the fundamental into the second harmonic wave leading to further decrease of the fundamental beam intensity. Thus the FDNLM introduces a negative nonlinear feedback and the FDNLM reflectivity decreases with increasing intensity of the fundamental beam, i.e. with increasing single pass SHG efficiency, see Fig. 3b. The proper adjustment of the value of  $\Delta\phi_{in}$  for specific FDNLM operation is realized by changing the distance between NLC and DM or by slightly rotating a glass plate placed between the NLC and DM. In both cases the dispersion in air and glass causes change in  $\Delta\phi_{in}$ . Originally the FDNLM was proposed first by Stankov<sup>16</sup> as a device based on perfectly phase-matched SHG.

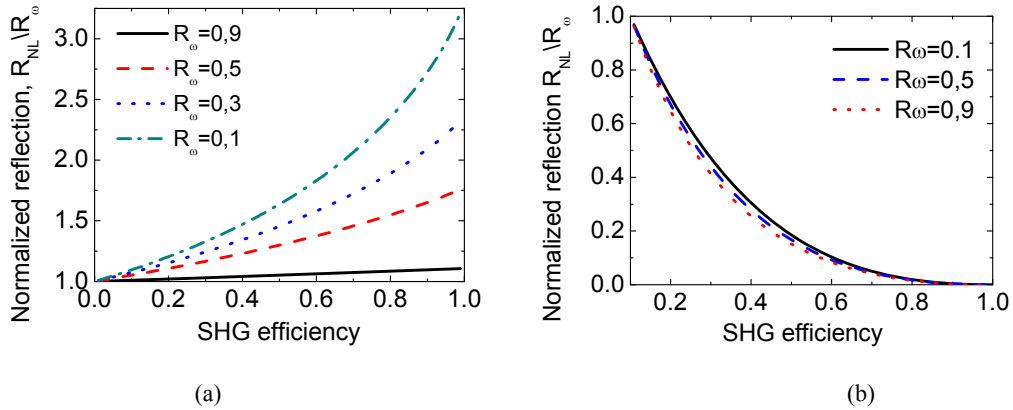


Fig. 3. Analytically calculated normalized FDNLM reflection as a function of the SHG efficiency for perfect phase matching and different  $R_{\omega}$ , (a)  $\Delta\varphi_{in} = \Delta\varphi_{out} \pm (2m+1)\pi$ ; (b)  $\Delta\varphi_{in} = \Delta\varphi_{out} \pm 2m\pi$ ,  $m=0,1,2\dots$

In the presence of phase-mismatch, the back conversion to the fundamental on the second pass through the nonlinear crystal depends on the phase shift  $\Delta\varphi$ , where  $\Delta\varphi$  is the wave vector mismatch, and  $L$  is the length of the SHG crystal. Hence, the intensity dependent reflection of the FDNLM is a function of the additional parameter  $\Delta kL$  which leads to new requirements for  $\Delta\varphi_{in}$  in comparison to the perfect phase matching case. Figure 4 shows  $R_{NL}$ , the normalized nonlinear reflection coefficient of the FDNLM, the pulse shortening ratio  $\rho = \tau_{in}/\tau_{out}$  equal to the pulse duration of the input pulse  $\tau_{in}$  divided by the reflected pulse duration  $\tau_{out}$ , and the nonlinear phase shift  $\varphi_1$  of the fundamental wave reflected by the FDNLM.

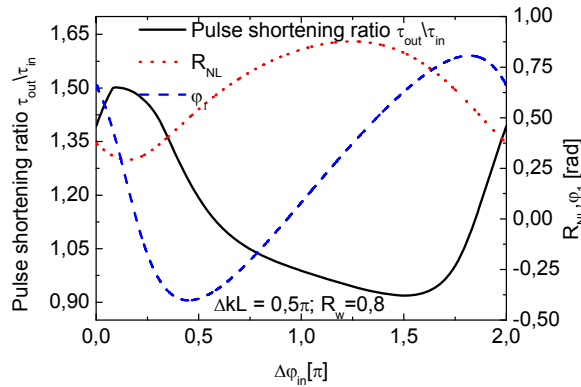


Fig. 4. Calculated pulse shortening ratio  $\rho = \tau_{in}/\tau_{out}$  (solid line), nonlinear reflection coefficient  $R_{NL}$  normalized to the linear reflectivity  $R_{\omega}$  of the dichroic mirror (dot line) and nonlinear phase shift  $\varphi_1$  of the fundamental wave (dash line), as functions of  $\Delta\varphi_{in}$ .

The numerical analysis in Fig.4 is performed within the plane-wave approximation assuming zero absorption. The corresponding coupled wave equations can be found elsewhere.<sup>14</sup> The parameters chosen are  $R_{\omega} = 80\%$  and  $U_{01} = 1$  where the normalized input amplitude  $u_{10}$  is defined by  $U_{01} = \sigma a_{01} L$ , with  $\sigma$  - the nonlinear coupling coefficient and  $a_{01}$  - the input amplitude. The magnitude of the pulse shortening as well as the actual existence of such pulse compression capability, depend primarily on  $\Delta\varphi_{in}$ . The pulse shortening is maximized when  $\Delta\varphi_{in}$  is between  $1.5\pi - 1.75\pi$  and this range remains in the vicinity of  $1.5\pi$  when the phase mismatch  $\Delta kL$  is varied between 0.3 and 1.5 rad.<sup>17</sup>

The second mode-locking mechanism is based on self-phase modulation of the fundamental wave, due to cascaded  $\chi^{(2)}$  nonlinearity, where the cavity losses are modified by the cascaded  $\chi^{(2)}$  lens formation. This leads to fundamental wave-front defocusing/focusing with intensity dependent focal length. The resulting lens in combination with appropriate hard

or soft aperture causes strongly nonlinear intracavity loss modulation and eventually leads to mode-locking. In contrast to the third order Kerr effect, where the resulting lens effect is only positive (i.e. focusing lens), in cascaded second order nonlinearity the lens type depends on the sign of the phase-mismatch  $\Delta kL$  and it can be “plus” which effects a negative or diverging lens and “minus” which effects a positive or converging lens. Also the cascaded nonlinear phase shift can be saturated. The saturation intensity depends on the phase mismatch parameter  $\Delta kL$  and its value increases when moving away from the perfect phase matching point. In contrast to the FDNLM technique the cascaded  $\chi^{(2)}$  lens mode-locking exists only for SHG at non-phase-matched condition, i.e. at  $\Delta kL \neq 0$ .

For better understanding of the cascading process and the way it leads to the phase shift, let us consider the case when a fundamental wave  $\omega$  is incident on a type-I nonlinear crystal with large second order nonlinearity. In non-phase-matched condition the power is continuously converted from the fundamental to the second-harmonic (up-converted) and from second-harmonic to the fundamental (down-converted) at every half coherence length ( $L_c/2$ ). A part of the initial fundamental wave is up-converted into second harmonic according to  $2\omega = \omega + \omega$  and the two waves travel with different phase velocity. After typically one half a coherence length, a part of the second harmonic is back-converted to the fundamental according to  $\omega_{bc} = 2\omega - \omega$  and the regenerated fundamental wave has different phase from the initial fundamental wave that has not been converted to second harmonic. Thus phase differences depends on the conversion efficiency and consequently on the intensity of the incident beam. If the radial distribution of the beam is not uniform, this will introduce curvature to the fundamental wave-front and the cascaded  $\chi^{(2)}$  process will act as a focusing or defocusing lens with intensity dependant focal length.

#### 4. EXPERIMENTAL RESULTS AND DISCUSSION

The phase matching of the intracavity PPKTP crystal is controlled by changing the crystal working temperature. The measured second-harmonic power versus temperature shows maximum conversion efficiency at  $60.5^\circ\text{C}$  (holder temperature) and  $\sim 12^\circ\text{C}$  FWHM of the temperature phase-matching curve (Fig. 5). Stable passive mode-locking operation is observed, however, at higher temperatures, around  $80^\circ\text{C}$ . The optimum temperature varied in an interval of  $\pm 4^\circ\text{C}$  for each experiment. A temperature induced phase-mismatch of  $\sim 6$  rad at  $80^\circ\text{C}$  is calculated using the temperature dependent Sellmeier equations for KTP.<sup>18</sup> Similar value of  $\sim 5.3$  rad is calculated using the ratio  $\theta = 0.27$  rad/ $^\circ\text{C}$  of the phase-mismatch coefficient, obtained by fitting the curve in Fig. 5 with  $\text{sinc}^2(\theta\Delta T)$ , where  $\theta\Delta T$  equals  $\Delta kL/2$

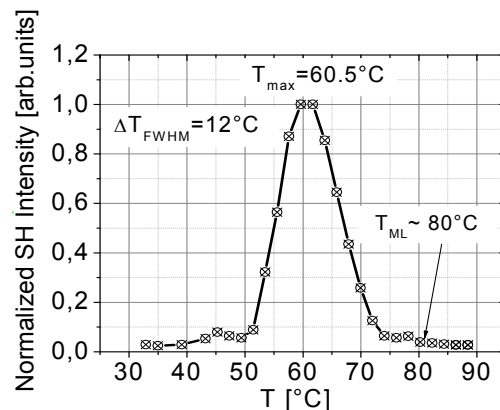


Fig. 5. Normalized second harmonic (SH) intensity as a function of the crystal holder temperature T

Mode-locked operation was studied with four different output couplers, three dichroic mirrors with partial reflectance (OC1 with 95%, OC2 with 80% and OC3 with 70%) at the fundamental wavelength and highly reflective for the second harmonic, and one output coupler, OC4 with partial reflectance (95%) at the fundamental and highly transmitting the second harmonic. The highest output power and efficiency in the mode-locking regime were achieved with the 30%-

transmitting output coupler. Figure 6 shows the dependence of the output versus the incident pump power. The laser threshold is 2.7 W. Passive mode-locking has been observed in two distinct pump power ranges, from 10 to 10.5 W and from 14.7 to 16.2 W. In both regions, the output power is decreasing while increasing the pump power. The modeling of the field distribution in the resonator shows two stability zones depending on the thermal lens in the Nd:YVO<sub>4</sub> active element. In the vicinity of the zone limits the mode size in the active elements is changing. Therefore the efficiency is dropping due to non-optimum overlapping with the pump beam.

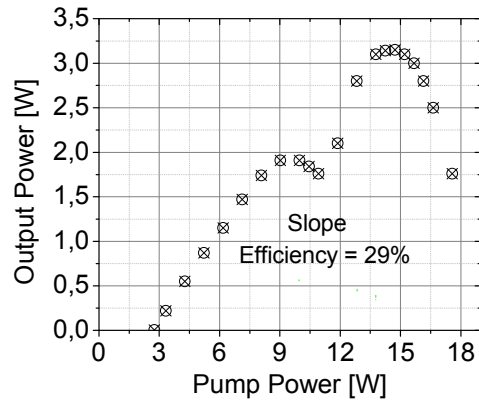


Fig. 6. Laser output power as a function of incident pump power.

The highest output power (3.1 W) in stable mode-locking regime is obtained at 15 W of incident pump power. In this case, the measured FWHM of the autocorrelation trace is 8 ps, Fig. 7a, which corresponds to pulse duration of 5.2 ps, assuming sech<sup>2</sup> pulse shape. The shortest pulse duration, 2.9 ps, see Fig. 7b, is obtained using the dichroic OC1 with 5% transmittance at the fundamental, highly reflecting at the second harmonic.

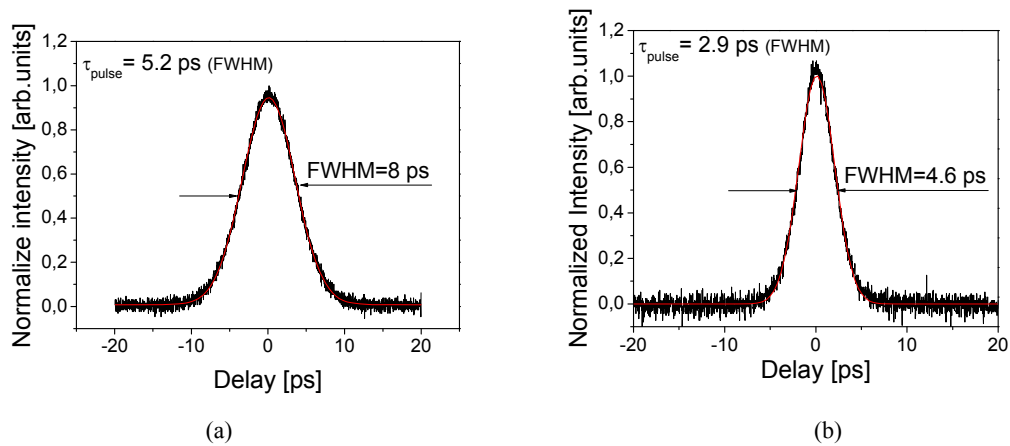


Fig.7. The autocorrelation functions (black curve) and fit assuming sech<sup>2</sup> pulse shape (red curve) using two different dichroic mirrors as an output coupler (a) for mirror OC3 - (b) for mirror OC1

The autocorrelation is measured by rotation–mirrors autocorelator using non-collinear second harmonic generation.

Successful mode-locking was achieved with all the three dichotic OCs with different transmission at the fundamental wavelength and high reflection at the second harmonic. In this case both nonlinear reflection and cascaded  $\chi^{(2)}$  lens process are simultaneously present. The nonlinear reflection of the FDNLM strongly depends on the phase-mismatch

and reaches a maximum level when the second harmonic is perfectly phase-matched. On the other side, cascaded  $\chi^{(2)}$  lens exists only if there is a phase-mismatch.

In order to analyze the relative contribution of the two mechanisms to the mode-locking process we suppressed the FDNLM effect by using the OC4 with the same reflectivity as OC1 at the fundamental but high transmission at the second harmonic. The laser threshold was the same as in the case of using OC1. The stable output power in the mode-locking regime amounted to 0.7 W, at a pump power of 10 W. The measured autocorrelation trace width is 7.2 ps. corresponding to pulse duration of 4.7 ps assuming sech<sup>2</sup> pulse shape. The mode locking displays amplitude fluctuations less than 2% on millisecond time scale and long term stability with hours of continuous operation.

The results from the characterization of the laser performance with the four OCs are summarized in Table 1.

Output coupler T% at 1064 nm & Reflectivity at 532 nm	OC1 5% & HR	OC2 20% & HR	OC3 30% & HR	OC4 5% & HT
Threshold pump power [W]	2.4	2.6	2.7	2.4
Slope efficiency [%]	6	27	29	9
Pump power range(s) with stable mode locking [W]	9 – 11 13.5	9 – 10.5 14.7 – 17.5	10 – 10,5 14.7 – 16.2	9 – 10.4 14
Output power [W]	<u>0.5 – 0.4</u> 1	1.9 – 1.8 <u>2.7 – 2.4</u>	1.9 – 1.8 <u>3.1 – 2.7</u>	<u>0.7 – 0.68</u> 1.1
Pulse duration (sech <sup>2</sup> shape) [ps]	<u>2.9</u>	<u>4.5</u>	<u>5.2</u>	<u>4.7</u>

Table 1. Summary of the laser performance with the four different output couplers

With each output coupler, mode-locking was obtained in regions of negative slope in the input-output power dependence, as those shown in Fig. 6 for OC3. The two regions of pump power correspond to the two rows of output power in the mode-locked regime. The underlined values for the output power correspond to the pulse durations given in the last row. At lower transmission of the output coupler at the fundamental (5% for OC1 and OC4) the self-sustained mode-locking is less stable in the higher power region. The optimum for mode-locking temperature of the crystal holder decreases by ~2°C. We attribute this behavior to the residual absorption in KTP and subsequent heating of the SHG crystal due to the increased average intracavity power. This effect requires more sophisticated temperature management system because KTP absorption mostly occurs at the second harmonic whose power strongly depends on the pulse length and thus changes dramatically when steady-state mode-locking is established and interrupted. Thus, the pulse duration values in Table 1 correspond to the output power range for which stable mode-locked operation was achieved.

## 5. CONCLUSION

We have demonstrated operation of a passively mode-locked Nd: YVO<sub>4</sub> laser by intracavity frequency doubling in PPKTP. The cascaded  $\chi^{(2)}$  lens mode-locking process is the dominant mechanism for pulse generation below 10 ps. Combination of the FDNLM technique with the cascaded  $\chi^{(2)}$  lens improves the long term stability and the self-starting capability of the system. Important result from the present study is the proof that stable mode-locking can be obtained up to the maximum output power achievable in the CW mode of operation.

## ACKNOWLEDGEMENTS

This work has been supported by the Bulgarian Ministry of Science and Education under NSF grants VU-L-319/2007 and DO 02/134/2009, Sofia University scientific research grant 294/2009, and DAAD (Germany) grant D/07/00333.

## REFERENCES

- [1] DeMaria, A. J., Stetser, D. A., and Heynau, H., "Self mode-locking of lasers with saturable absorbers," *Appl. Phys. Lett.* 8(7), 174-176 (1966).
- [2] Keller, U., "Recent developments in compact ultrafast lasers," *Nature* 424(6950), 831-838 (2003).
- [3] Cerullo, G., De Silvestri, S., Monguzzi, A., Segala, D., and Magni, V., "Self-starting mode-locking of a CW Nd-YAG laser using cascaded second-order nonlinearities," *Opt. Letters* 20(7), 746-748 (1995).
- [4] Agnesi, A., Lucca, A., Reali, G., and Tomaselli, A., "All-solid-state high-repetition-rate optical source tunable in wavelength and in pulse duration," *J. Opt. Soc. Am. B* 18(3), 286-290 (2001).
- [5] Keller, U., Weingarten, K. J., Kärtner, F. X., Kopf, D., Braun, B., Jung, I. D., Fluck, R., Hönninger, C., Matuschek, N., and Aus der Au, J., "Semiconductor saturable absorber mirrors (SESAM's) for femtosecond to nanosecond pulse generation in solid-state lasers," *IEEE J. Sel. Top. Quant. Elec.* 2(3), 435-453 (1996).
- [6] Graf, T., Ferguson, A. I., Bente, E., Burns, D., and Dawson, M. D., "Multi-Watt Nd:YVO<sub>4</sub> laser, mode locked by a semiconductor saturable absorber mirror and side-pumped by a diode-laser bar," *Opt. Commun.* 159(1-3), 84-87 (1999).
- [7] Burns, D., Hetterich, M., Ferguson, A. I., Bente, E., Dawson, M. D., Davies, J. I., and Bland, S. W., "High-average-power (> 20-W) Nd:YVO<sub>4</sub> lasers mode locked by strain-compensated saturable Bragg reflectors," *J. Opt. Soc. Am. B* 17(6), 919-926 (2000).
- [8] Chen, Y. F., Tsai, S. W., Lan, Y. P., Wang, S. C., and Huang, K. F., "Diode-end-pumped passively mode-locked high-power Nd:YVO<sub>4</sub> laser with a relaxed saturable Bragg reflector," *Opt. Letters* 26(4), 199-201 (2001).
- [9] Chen, Y. F., Tsai, S. W., and Wang, S. C., "High-power diode-pumped nonlinear mirror mode-locked Nd:YVO<sub>4</sub> laser with periodically-poled KTP," *Appl. Phys. B* 72(4), 395-397 (2001).
- [10] Agnesi, A., Pennacchio, C., Reali, G. C., and Kubecek, V., "High-power diode-pumped picosecond Nd<sup>3+</sup>:YVO<sub>4</sub> laser," *Opt. Letters* 22(21), 1645-1647 (1997).
- [11] Buchvarov, I. C. and Saltiel, S. M., "Passive feedback control of actively mode-locked pulsed Nd:YAG laser," *Proc. SPIE* 1842, 124-129 (1992).
- [12] Buchvarov, I. C., Stankov, K. A., and Saltiel, S. M., "Pulse shortening in an actively mode-locked laser with a frequency-doubling nonlinear mirror," *Opt. Commun.* 83(3-4), 241-245 (1991).
- [13] Stankov K. A. and Jethwa, J., "A new mode-locking technique using a nonlinear mirror " *Opt. Commun.* 66(1), 41-46 (1988).
- [14] Buchvarov, I., Christov, G., and Saltiel, S., "Transient behavior of frequency doubling mode-locker. Numerical analysis," *Opt. Commun.* 107(3-4), 281-286 (1994).
- [15] Holmgren, S. J., Pasiskevicius, V., and Laurell, F., "Generation of 2.8 ps pulses by mode-locking a Nd:GdVO<sub>4</sub> laser with defocusing cascaded Kerr lensing in periodically poled KTP," *Opt. Express* 13(14), 5270-5278 (2005).
- [16] Stankov, K. A., "A mirror with an intensity-dependent reflection coefficient," *Appl. Phys. B* 45(3), 191-195 (1988).
- [17] Gaydardzhiev, Stalnikov, A., and Buchvarov, I., "Generation of a train of ps-pulses from a diode pumped Nd-laser using electro-optical negative feedback," presented at the International Conference on Ultrafast and Nonlinear Optics UFNO'2009, Sep. 14-18, Burgas, Bulgaria, 2009, Paper UFL-P6, Book of Abstracts, p12.
- [18] Kato, K. and Takaoka, E., "Sellmeier and thermo-optic dispersion formulas for KTP," *Appl. Optics* 41(24), 5040-5044 (2002).